Journal of Applied Mathematics and Physics, 2022, 10, 3530-3547
https://www.scirp.org/journal/jamp
ISSN Online: 2327-4379
ISSN Print: 2327-4352

The Mathematical Thoughts and Physics Interpretations of Rainbow from Ancient to Modern Times

Ariel Wu

Beijing Number 4 High School, Beijing, China
Email: ariel110911091109@163.com

How to cite this paper: Wu, A. (2022) The Mathematical Thoughts and Physics Interpretations of Rainbow from Ancient to Modern Times. *Journal of Applied Mathematics and Physics*, **10**, 3530-3547.
https://doi.org/10.4236/jamp.2022.1012234

Received: October 1, 2022
Accepted: December 6, 2022
Published: December 9, 2022

Abstract

With the aim of building a more precise mathematical model of better predictability for the formation of the supernumerary rainbow and fogbow and seeking a clearer and more elaborate physical interpretation, this paper examines the relationship between different rainbow patterns and droplet sizes through both analytical derivation and numerical simulation and develops a much more detailed model beyond previous explanations. From Newton's geometric model of optics to Young's wave model, the paper first establishes a solid foundation for the understanding of the formation of the rainbow in nature and through human vision, and then goes on examining the interferences of light, finally applying the model in reality for a better understanding of complex rainbow phenomena, with additional analysis on an unexpected finding about the correspondence of maximum view angle and shortest light path through hypothetical explanation based on the principle of least time and simulation of an elliptical droplet.

Keywords

Rainbow, Optics, Interference, Supernumerary Rainbow, Fogbow, Light Path

1. Introduction

Rainbows have long been appreciated as a marvel of nature too wondrous to be explained and understood by mankind. Yet, throughout history, there has always existed a small group of people unsatisfied with the idea that explained rainbow thinly by the advent of deity. From the science of human vision to the understanding of how light travels and behaves, the process of "unweaving the rainbow" has made its progress gradually. Sir Isaac Newton (**Figure 1**) provided us

with the first integrated theory of the rainbow [1]. The phrase "unweaving the rainbow" is coined by poet John Keats who defied Newton's work of demystifying the rainbow using science and therefore diminishing its wonder [2]. Nevertheless, the work of Newton offered that small group of people an explanation more than poetic.

This paper aims to first provide its readers with a thorough exposition of the rainbow based on pre-Newton and Newton's basic theory of geometric model of optics, elaborating on several key elements of how the rainbow is viewed in the way it is. Then the paper goes further beyond the geometric model to the wave-like description of optics, first developed by Thomas Young (**Figure 2**) [3], analytically and numerically deriving the superposition pattern of the rainbow and

Figure 1. Isaac Newton.

Figure 2. Thomas Young.

offering a satisfactory explanation of the less commonly seen but more mysterious optical phenomena: the supernumerary rainbow and the fogbow. Finally, examining an interesting coincidence that arises during the course of this work, the paper will offer an insight into the relation between the geometric model and the wave model primarily based on path integral developed by Richard Feynman [4].

2. Geometric Model

This section of the paper provides the basic principles of the rainbow based on the geometric model of optics. Beginning with a brief overview based on ray tracing within a single droplet, the paper then goes deeper explaining the math behind the visual characteristics of the rainbow, and finally moves to explain the relationship between the optical pattern formed by a single droplet and the rainbow by a collection of droplets from the observer's perspective.

2.1. Single Droplet Model

The formation of the rainbow has several requirements: First, the sun has to be at the back of the observer; second, there must be water droplets in front of the observer; third, there's no obstruction to the light path. These ingredients must all be present because the rainbow is essentially formed by the light coming from the back of the observer passing through a collection of droplets ahead of the observer, then raying back to the observer's eyes after dispersion (two times of refraction and one time of reflection) through droplets.

Figure 3 [5] provides the basic settings of a single droplet model, labeling variables that are used throughout the paper.

Since the refractive index of water changes with the wavelengths of light, sunlight (white light) undergoes so-called dispersion through the droplet. Dispersion is essential to the manifestation of a rainbow. For every single droplet, as parallel light rays of each wavelength hit the droplet (with the sun seen as an

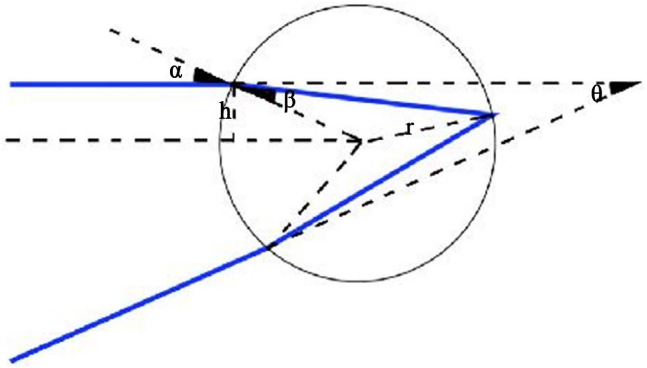

α : incident angle; β : refracted angle; r: droplet radius; h: height, relative position of the incident ray; x: $\sin\alpha$, which can also be understood as the ratio of height h to radius r; λ : wavelength; n: refractive index in water; θ : view angle, angle between the incident ray into the droplet and the exit ray out of it.

Figure 3. Single droplet model.

infinitely distant point source), the view angle θ is expressed as a function of x, the sin of incident angle α, in [EQ-view angle], as derived through basic geometric skills and trigonometry, presented in Figure 3. As shown in Figure 4, the function first increases and then decreases. The maximum view angle θ_0 corresponds to x_0.

[EQ-view angle]

$$\theta(x) = 4\arcsin\frac{x}{n} - 2\arcsin x \tag{1}$$

2.2. Maximum View Angle

Since the view angle θ changes at a low rate when x is close to the critical value x_0, as shown in Figure 4, the exit rays from the droplet concentrate at the maximum view angle θ_0, as demonstrated in Figure 5. Therefore, it is typically mostly the exit light at the maximum view angle that is visible to the naked eye.

Light rays of different wavelengths have different refractive index in water and thus will exit from the droplet at different values of the maximum view angle. Figure 5 only displays the rays of a specific wavelength ($\lambda = 0.45$ μm, with refractive index $n = 1.34055$) entering the droplet through the upper half, since these rays are the ones typically responsible for forming the rainbow to the observer. The 3D spherical construction of the same droplet could easily be generated by rotating the 2D circle about the horizontal axis passing through the center of the droplet. Thus, light rays of a single wavelength from a droplet form a cone in 3D space, with a concentration of light at the outermost layer of the cone, corresponding to the maximum view angle, as shown in Figure 6. Overlaying the cones of the exit rays of different wavelengths together produces a super cone, within which the superposition of light of all wavelengths forms a white color. Individual colors only appear at the outermost layers of each cone that makes up the super cone, due to the concentration of exit light at the maximum view angle.

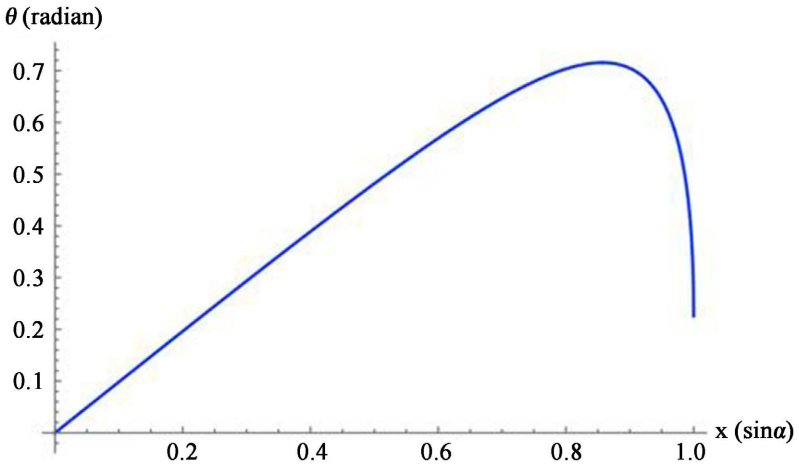

Figure 4. View angle function graph (wavelength $\lambda = 0.45$ μm, refractive index $n = 1.34055$, radius $r = 10$ μm).

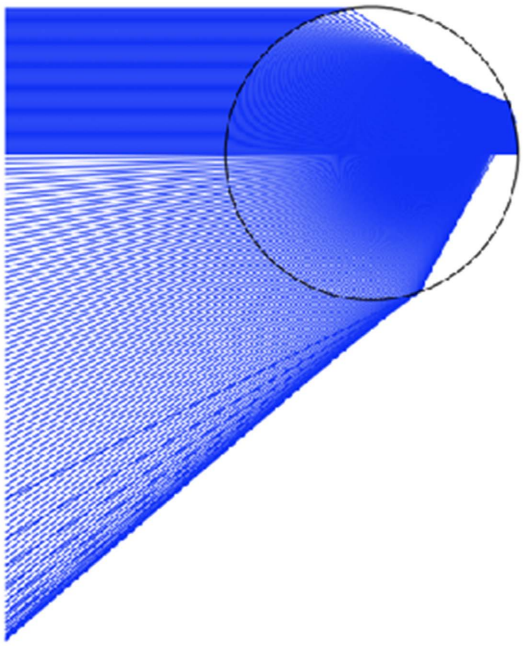

[Footnote: This paper relies on Mathematica for generating interactive demonstrations, of which we display some representative snapshots as figures in the paper. The code incorporates arrays matching the different wavelengths to their refractive index in water, using an RGB color scheme so that the generated graphs match exactly with the real scenario. The interactive programs allow users to independently choose different initial parameters and generate the outcomes. The program can be accessed through Mathematica's published pages, at the following URL https://www.wolframcloud.com/obj/ariel110911091109/Published/Unweaving the Rainbow by Ariel Wu.nb.]

Figure 5. Maximum view angle.

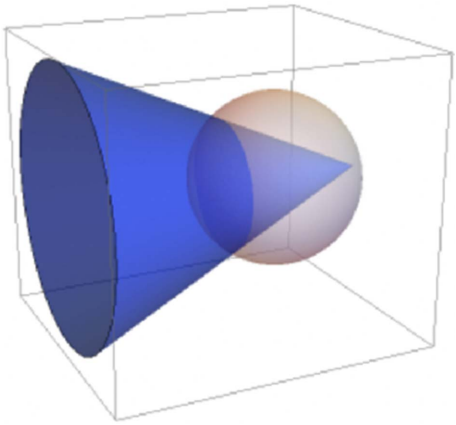

Figure 6. Single cone model.

2.3. Observer's Perspective

From the above account, a single droplet can form a rainbow-like pattern by projecting its exit light on the wall. Yet, it is still not the same as the natural phenomenon of a rainbow, which is formed by light directly beaming into the observer's eyes rather than a projection, and as such it requires a collection of

droplets rather than a single one. The reason why the real rainbow looks exactly like the rainbow-like pattern formed by a single droplet is that the sight angle θ' [angle between sunlight and the angle of sight] is essentially the same as view angle θ due to simple geometry. Thus, the cone of sight from the observer is no different than the cone of exit light from every single droplet, except the former receives light while the latter generates light. The cone of sight gives rise to the rainbow viewed by each observer individually. At each sight angle θ' matching with a maximum view angle θ for light of a certain wavelength, the observer sees the corresponding exit light coming from all the droplets aligned at the angle of sight (again, a cone). A row on the cone is shown in Figure 7 to demonstrate the idea.

The following sections of the paper will not specifically distinguish between view angle θ and sight angle θ' since they are essentially equivalent to each other.

3. Wave Model

The above analysis is still all based on the geometric model of optics. Though it satisfactorily explains the formation of a typical rainbow, for more complex phenomena such as supernumerary rainbow and fogbow, shown in Figure 8 and Figure 9, the geometrical model is not adequate [6]. Not until Thomas Young's wave theory of light was introduced and validated, did these phenomena become understood as resulting from the superposition of light (electromagnetic) waves. Through analytical and numerical modeling, the superposition pattern is found to depend on the size of the droplet, giving a more quantitative and precise account of the more complex realizations of the rainbow.

3.1. Light Path and Phase Change

The use of wave theory requires the calculation of the phase change for each

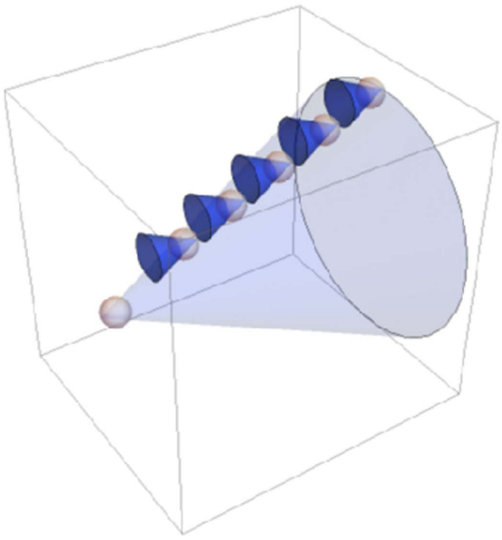

Figure 7. Observer model.

Figure 8. Supernumerary rainbow.

Figure 9. Fogbow.

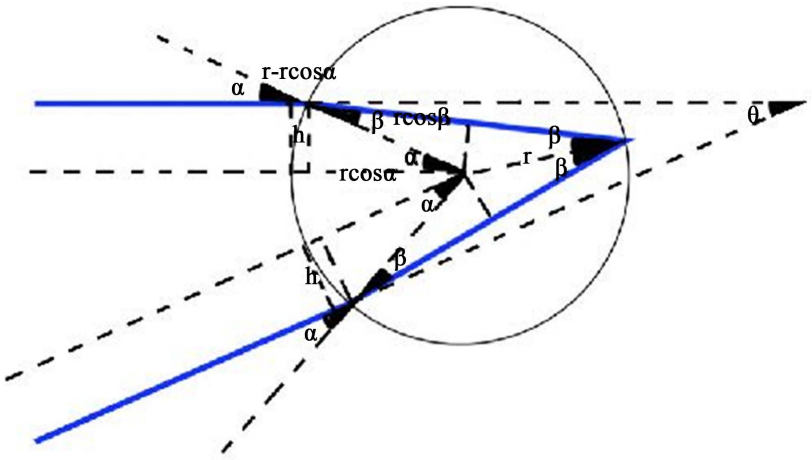

Figure 10. Phase change graph.

incident ray, shown in Figure 10 [7], which is later used for deriving the superposition pattern of higher order maxima. Here, the path distance is defined as the index of refraction times the distance that light travels; the phase change is the path difference times $2\pi/\lambda$. Notice that the path distance here is defined by comparing two light rays both entering and exiting the droplet along parallel directions.

d_{out} -path distance outside the droplet

$$d_{out} = 2(r - r\cos\alpha)$$

d_{in} -path distance inside the droplet

$$d_{in} = 4r\cos\beta$$

ϕ_{out} -phase change outside the droplet

$$\phi_{out} = \frac{2\pi}{\lambda} d_{out} = \frac{2\pi}{\lambda} 2(r - r\cos\alpha)$$

ϕ_{in} -phase change inside the droplet

$$\phi_{in} = \frac{2\pi}{\lambda} n d_{in} = \frac{2\pi}{\lambda} n4r\cos\beta$$

$\phi(x)$ -overall phase change

[EQ-overall phase change]

$$\phi(x) = 4\pi\left(\frac{r}{\lambda}\right)\left(1 - \sqrt{1-x^2} + 2\sqrt{n^2 - x^2}\right) \tag{2}$$

[EQ-overall phase change] gives the overall phase change ϕ of an incident light wave expressed in terms of *x*. As *x* increases, the overall phase change ϕ first decreases and then increases, as shown in Figure 11. Interestingly, the minimum of the overall phase change (same for the overall path distance) corresponds to the light path of the maximum view angle. This intriguing correspondence will be explored further in section 4.

3.2. Superposition (Analytical)

In order to derive the superposition pattern, we want to identify the incident light waves that come out at the same view angle—the same angle viewed by the observer's eye—and then check if the corresponding exit light waves interfere constructively or destructively.

To reach the first goal, we have to calculate the two solutions for the same view angle using **[EQ-view angle]**. For the convenience of calculation, we expand the expression for the maximum view angle into a Taylor series up to the

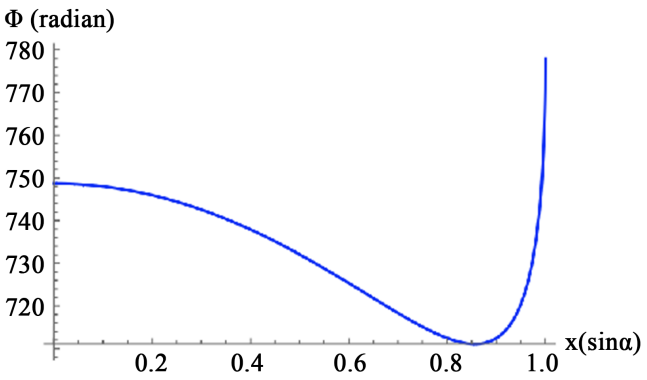

Figure 11. Overall phase change function graph (wavelength $\lambda = 0.45\,\mu m$, refractive index $n = 1.34055$, radius $r = 10\,\mu m$).

3rd order as **[EQ-view angle Taylor Series]**. As explained in the first section, the closer to the maximum view angle, the more intense the exit light. Thus, we justify the approximation by assuming that only exit rays not too far from the maximum view angle contribute to the part of the supernumerary rainbow via superposition.

[EQ-view angle]

$$\theta(x) = 4\arcsin\frac{x}{n} - 2\arcsin x \tag{3}$$

[EQ-view angle Taylor Series]

$$\theta(x_0) = 4\arcsin\frac{x_0}{n} - 2\arcsin x_0$$

$$\theta'(x_0) = \frac{4}{\sqrt{n^2 - x^2}} - \frac{2}{\sqrt{1 - x^2}} = 0$$

$$x_0 = \frac{\sqrt{4 - n^2}}{\sqrt{3}}$$

$$\theta''(x_0) = -\frac{9}{2}\frac{\sqrt{4 - n^2}}{\left(n^2 - 1\right)^{\frac{3}{2}}}$$

$$\theta(x) \approx \theta(x_0) + \frac{1}{2}\theta''(x_0)(x - x_0)^2$$

$$\theta(x) \approx \left(4\arcsin\frac{x_0}{n} - 2\arcsin x_0\right) - \frac{9\sqrt{4 - n^2}}{4\left(n^2 - 1\right)^{\frac{3}{2}}}(x - x_0)^2 \tag{4}$$

Since the view angle function can be approximated as a quadratic function near its maximum, the two solutions of a certain view angle below the maximum are symmetric with respect to $y = x_0$. Thus, we find that the two incident light entering the droplet at $x_0 + \Delta x$ and $x_0 - \Delta x$ have the same view angle, shown in **[EQ-same view angle]**.

[EQ-same view angle]

$$\theta(x_0 + \Delta x) = \theta(x_0 - \Delta x) \tag{5}$$

For the second part of the calculation—determining whether the two light waves existing at the same view angle interfere constructively or destructively—we have to use the function describing the overall phase change. If the two light waves differ in phase by an integer multiple of 2π, they will interfere constructively. Again, using Taylor Series to its third order for the overall phase change function **[EQ-overall phase change]**, we get **[EQ-overall phase change Taylor Series]**.

[EQ-overall phase change]

$$\phi(x) = 4\pi\left(\frac{r}{\lambda}\right)\left(1 - \sqrt{1 - x^2} + 2\sqrt{n^2 - x^2}\right)$$

[EQ-overall phase change Taylor Series]

$$\phi(x) \approx \phi(x_0) - 2\pi\left(\frac{r}{\lambda}\right)\left(\frac{1}{3}\theta''(x-x_0)^3 + \frac{1}{2}\theta'' x_0 (x-x_0)^2\right) \tag{6}$$

We want to compute the difference in the overall phase change of the two light waves that exit at the same view angle. As we have already found out, the light entering at $x_0 + \Delta x$ and $x_0 - \Delta x$ will exit at the same view angle. After plugging the same two values into the overall phase change function, we can calculate their difference and figure out the result under the condition that the difference is an integer multiple of 2π, shown in **[EQ-phase change difference]**.

[EQ-phase change difference]

$$\phi(x_0 + \Delta x) - \phi(x_0 - \Delta x) = -2\pi\left(\frac{r}{\lambda}\right)\left(\frac{2}{3}\theta''(x_0)\Delta x^3\right) = 2\pi[\text{integer}] \tag{7}$$

Since we want to find out how the view angle is dependent on the size of droplet, we can substitute Δx^3 in **[EQ-phase change difference]** by deriving it from the view angle function **[EQ-view angle Taylor Series]** we already have and get the final expression of view angle in terms of the droplet size.

[EQ-correlation between view angle and droplet size]

$$\theta(x) - \theta(x_0) \approx \frac{1}{2}\theta''(x_0)(x-x_0)^2$$

$$(x-x_0)^3 = \Delta x^3 \approx \left(\frac{2(\theta(x)-\theta(x_0))}{\theta''(x_0)}\right)^{\frac{3}{2}}$$

$$[\text{integer}] \approx -\left(\frac{r}{\lambda}\right)\left(\frac{2}{3}\theta''(x_0)\left(\frac{2(\theta(x)-\theta(x_0))}{\theta''(x_0)}\right)^{\frac{3}{2}}\right)$$

$$\theta(r) \approx \theta(x_0) - \frac{3}{4\sqrt{2}}(\theta''(x_0))^{\frac{1}{3}}\left(\frac{\lambda}{r}\right)^{\frac{2}{3}}[\text{integer}]^{\frac{2}{3}} \tag{8}$$

Thus, at a certain wavelength, the view angle for the constructive interference (corresponding to a maximum of the supernumerary) can directly be expressed as a function of the droplet radius.

3.3. Superposition (Numerical)

The numerical treatment of the same problem is more accurate than the Taylor Approximation. In addition, it is able to not just be restricted to conditions of constructive (or destructive) interference, but can rather generate a more complete superposition pattern based on the continuous phase change difference ΔΦ for each pair of incident rays in general. We take the same values of both the wavelength of the incident light and the corresponding refractive index as used previously (wavelength $\lambda = 0.45\ \mu\text{m}$, refractive index $n = 1.34055$, radius $r = 10\ \mu\text{m}$).

First, to find the two light waves that exit the droplet at the same view angle, we generate a pair of solutions (in terms of *x*) for each input value of the view angle. Instead of approximating the function as symmetric around the maximum, we can generate the exact values of the two solutions x_1 and x_2, as shown

in Figure 12.

The range of view angles is restricted from 0.6 radian to its maximum 0.714 radian since light coming out at an even lower view angle would be too weak to be seen. Here, we insert x_1 and x_2 respectively into the expression for the overall phase change and then calculate the difference for the two light waves that come out at the same view angle.

Again, if the phase change difference is an integer multiple of 2π, then the two light waves must add up as constructive interference maxima. Yet, instead of only matching the values to the condition of constructive interference, we construct a function to examine the variation of phase difference, which also provides a complete view of the superposition pattern around the maximum view angle, as expressed in **[EQ-superposition cos function]**.

[EQ-superposition cos function]

$$f(x) = \cos\frac{1}{2}\Delta\phi$$

The function graph of $\cos\frac{1}{2}\Delta\phi$ is generated as the function of the view angle θ, shown in Figure 13. The peak represents the central maxima of constructive interference, the zero represents the minima of destructive interference, and

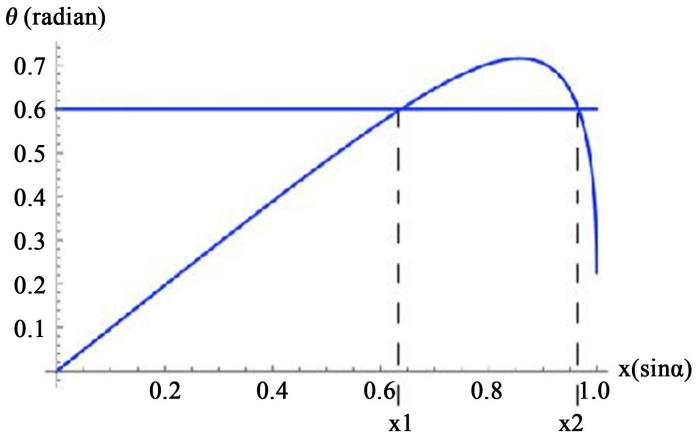

Figure 12. Numerical solutions for incident lights.

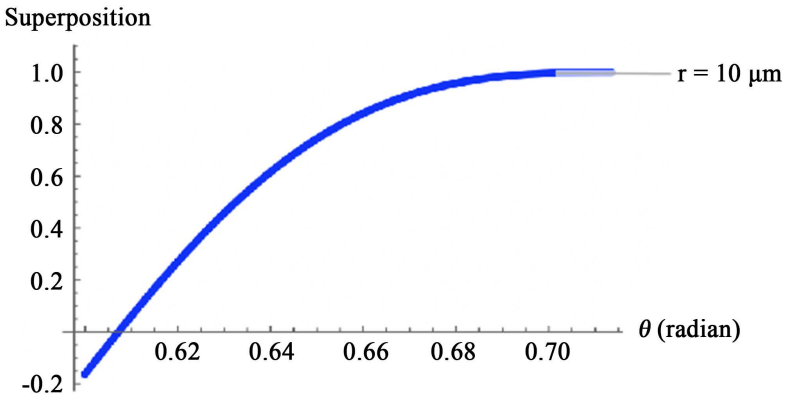

Figure 13. Superposition cos function graph.

the trough that could occur at a view angle lower than 0.6 radian represents the first order maxima. Each plot point can be traced back to a certain view angle input in the first step, thus describing a complete superposition pattern.

4. Interesting Correspondence

An interesting observation was made during the course of this analysis. As suggested above, the light path that exits the droplet at the maximum view angle—the light path most visible to the naked eye due to concentrated intensity—happens to be the one with the shortest path distance and thus the shortest travel time.

4.1. The Phenomenon

With the functions of the view angle and the light path compared in Figure 14, it appears that the two extrema are coincident (sane value of x), more apparently shown by the relationship that the two derivatives are the multiple of each other.

Fermat's Principle claims that light travels along the path that takes the shortest time in geometric optics, which is a classical approximation of Feynman's quantum mechanical path integral approach [8]. While the principle of least time is responsible for explaining why each individual light ray follows its path through the droplet, it still can't explain why collectively light rays concentrate at the maximum view angle, which is the shortest light path among all possible.

The path integral formulation gives a deeper explanation for the unique light path in the classical model. It states that each and every possible path contributes

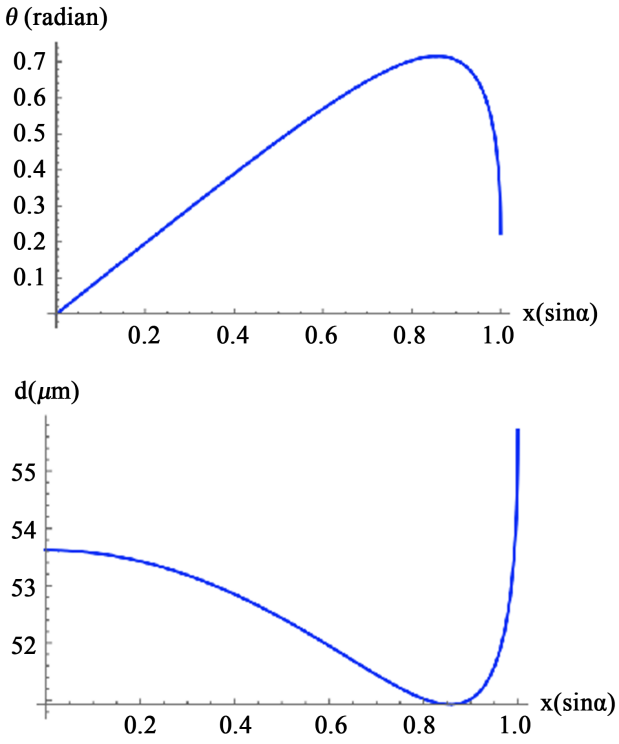

Figure 14. View angle function & path distance function.

to the overall result of light amplitude, and the largest contribution comes from the classical path.

4.2. Hypothetical Explanation

This paper offers a hypothetical explanation of the above phenomenon again using Feynman's path integral approach [4]: all light incidents into the droplet constitute another path integral. The light paths that contribute the most to the overall light wave propagating through the droplet gather at the maximum view angle. Overall, the path integral method is used twice, the first one decides the light path of each light ray, and the second one decides the concentration of light paths among all possible.

The paper examines the phenomenon in an elliptical droplet using the same approximation for light rays entering and exiting the droplet parallel (the condition for interference) [9]. The simulation indicates that there is still a maximum view angle where all light is concentrated, as shown in **Figure 15**; however, as the view angle increases and then decreases with the increase of entering height, the path distance increases only, which should be intuitive with the shape of ellipse. This indicates that the spherical-shaped droplet is unique in the phenomenon.

5. Conclusions and Discussions

This section of the paper offers the final conclusions from the above research and proposes some potential questions to it.

5.1. Physical Interpretation

This section offers a physical interpretation of the mathematical results derived

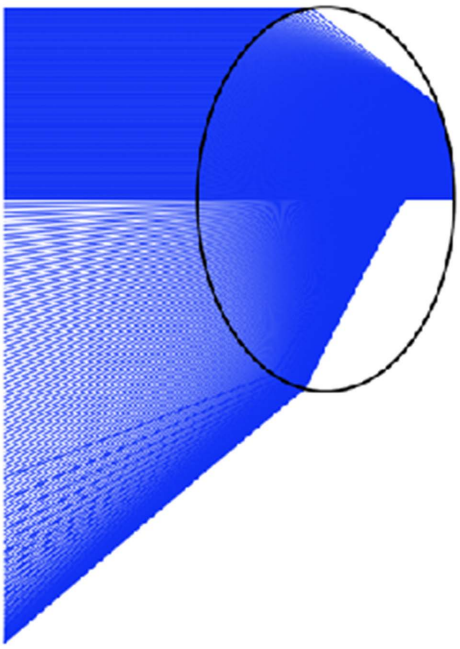

Figure 15. Elliptical droplet.

above and explains the formation of the supernumerary rainbow, the fogbow, and the typical rainbow. Superposition of light waves is always present; however, whether it is visible to the human eye primarily depends on the droplet size.

[EQ-correlation between view angle and droplet size]

$$\theta(r) \approx \theta(x_0) + \frac{3}{4\sqrt{2}}\left(\theta''(x_0)\right)^{\frac{1}{3}}\left(\frac{\lambda}{r}\right)^{\frac{2}{3}}[\text{integer}]^{\frac{2}{3}}$$

$$\text{with } x_0 = \frac{\sqrt{4-n^2}}{\sqrt{3}}$$

$$\theta(x_0) = 4\arcsin\frac{x_0}{n} - 2\arcsin x_0$$

$$\theta''(x_0) = -\frac{9}{2}\frac{\sqrt{4-n^2}}{\left(n^2-1\right)^{\frac{3}{2}}}$$

Applying the final analytical result of the superposition pattern in **[EQ-correlation between view angle and droplet size]**—view angle expressed in terms of droplet radius—we first insert a specific wavelength and its corresponding refractive index into the expression (again, wavelength $\lambda = 0.45\ \mu\text{m}$, refractive index $n = 1.34055$), the pattern of which essentially represents that of the entire visible spectrum of continuous wavelengths. Here, we generate the following equations for first, second, and third order maxima respectively, shown as **[EQ-1st, 2nd, and 3rd maxima view angle for special values]**.

[EQ-1st, 2nd, and 3rd maxima view angle for special values]

first order maxima: $\theta(r) \approx 0.71546 - 0.65691r^{-\frac{2}{3}}$

second order maxima: $\theta(r) \approx 0.71546 - 1.04278r^{-\frac{2}{3}}$

third order maxima: $\theta(r) \approx 0.71546 - 1.36643r^{-\frac{2}{3}}$

Since this is a model applied to the real world, we look at the droplet sizes that can be formed in reality [10]. The droplets can be classified into four types according to their sizes, shown in Figure 16.

With the range of droplet size known, we can generate function graphs for the first, second, and third order maxima view angle respectively according to

Type	Size
Dry Fog	Under 10 μm
Fine Fog	10-100 μm
Fine Drizzle	100-300 μm
Light Rain	300-1000 μm
Rain Storm	Over 1000 μm

Figure 16. Droplet size classification.

[EQ-1st, 2nd, and 3rd maxima view angle for special values]. Separating the range into 10 - 100 μm, 100 - 300 μm, and 300 - 1000 μm, we can see how the view angles of the first three orders of maxima are getting larger and larger, and therefore closer and closer to the maximum view angle (at central maxima). However, the rate of increase is getting much and much slower, that the first 100 μm of change in radius generates most of the change in view angle through the entire range, shown in the change of function value in Figure 17.

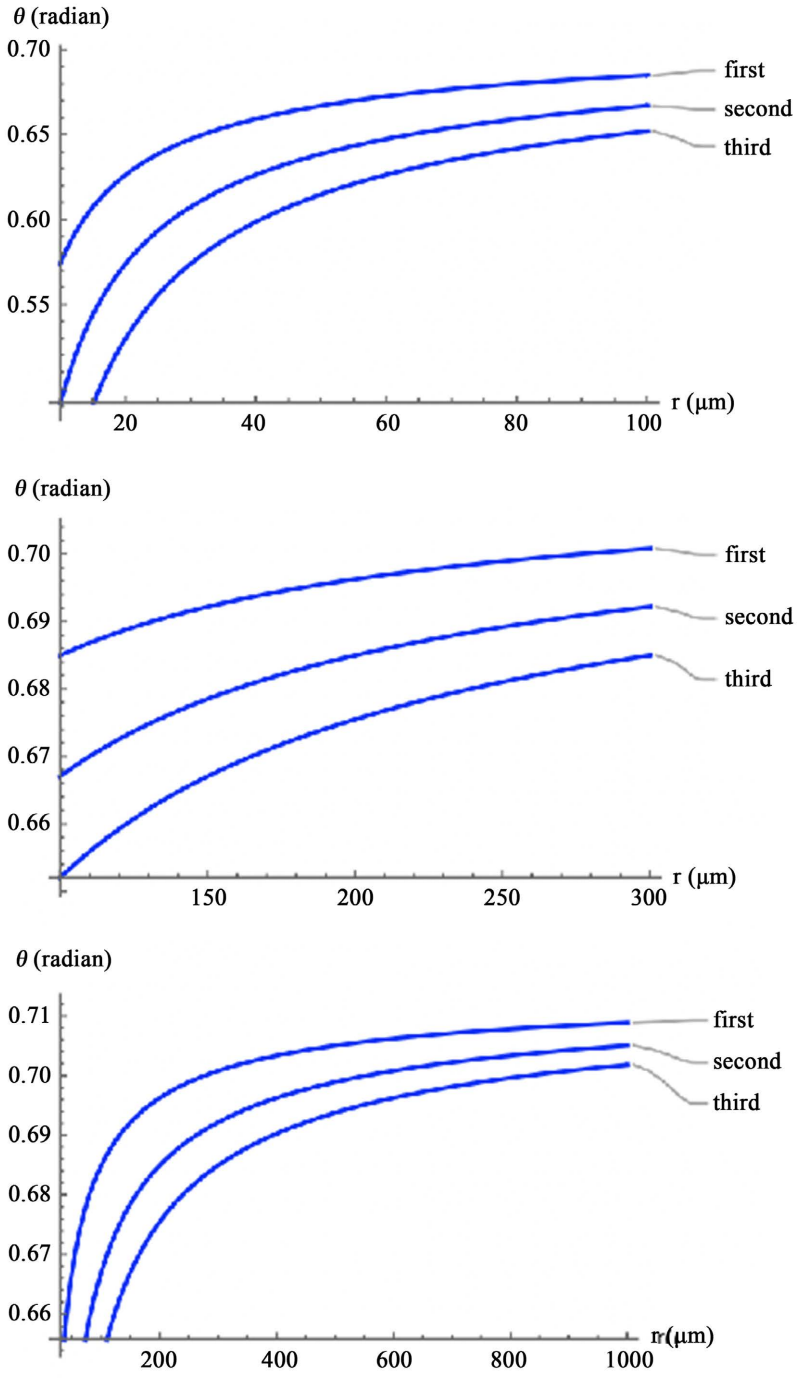

Figure 17. 1st, 2nd, and 3rd maxima view angle from 10 - 100 μm, 100 - 300 μm, 300 - 1000 μm.

We can also use the numerical treatment, which generates the complete pattern of superposition with each different radius value input. Here, Figure 18 shows the complete superposition pattern of $r = 10\ \mu m$, $r = 100\ \mu m$, and $r = 300\ \mu m$ at view angle from 0.600 to 0.714. While the 10 μm droplet radius case does not even reach its first order maxima within the view angle range, the 100 μm droplet radius case already reaches its fifth maxima and the 300 μm one even more.

With the superposition patterns of different droplet sizes generated above, we can now try to understand how our model explains the physical characteristics of different phenomena. For the superposition pattern to be visible (assuming there is no obstruction to sight) by the naked eye, two conditions need to be met: 1) the higher order interference pattern can not be too close to the central maxima to be distinguished; 2) the higher order interference pattern can not be too far from the central maxima or the light would be too weak.

To meet the first condition, the view angle difference between the first order maxima and the central maxima has to exceed the view angle difference of the rainbow's two fringes (that is to say, the angle of the first order red has to exceed that of the primary violet, with red light of wavelength $\lambda = 0.65\ \mu m$ and refractive index $n = 1.33257$, and violet light of wavelength $\lambda = 0.40\ \mu m$ and refractive index $n = 1.34451$). Inputting the parameters, the view angle difference of red light and violet light has a view angle difference of approximately 0.03 radian.

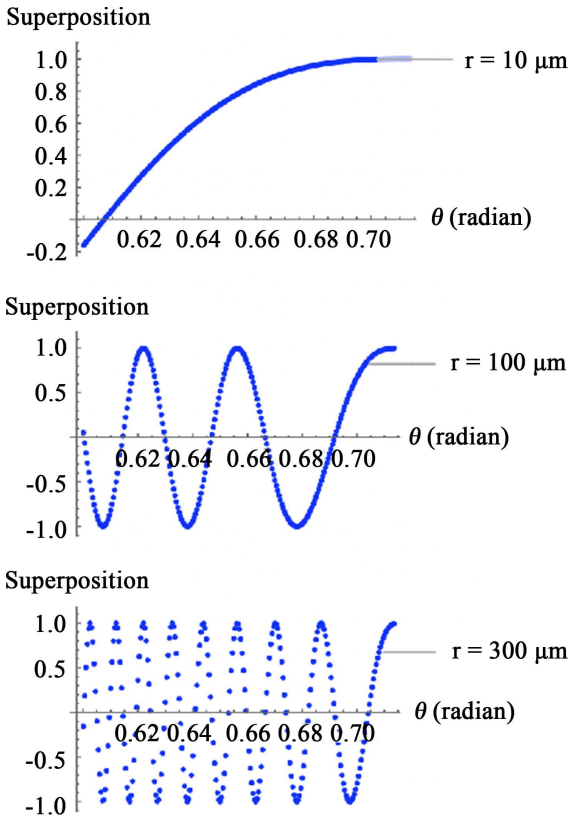

Figure 18. Superposition pattern at view angle 0.600 - 0.714 radian (maximum view angle), for $r = 10\ \mu m$, $r = 100\ \mu m$, and $r = 300\ \mu m$.

This means that the light has to have a view angle smaller than 0.684 radian in our case, which, as shown in Figure 17 directly, is only possible when the radius of the droplet is smaller than 100 μm. Thus, any rainbow generated by droplets with a radius larger than 100 μm will have its first and second order of maxima all overlapped with the central maxima and thus can not be seen directly—which is how a typical rainbow is generated. If the droplet radius almost meets the condition and does not generate the first maxima completely overlapped with the central maxima, a partial overlap of light at the fringe can be seen, as shown in Figure 8 that a purple-pink color is generated by the overlapping of violet light of the central maxima and the red light of the first order maxima.

Then, to meet the second condition, the first maxima can not be too far away from the maximum view angle, or the light would be too weak. As stated above, generally, the closer to the maximum view angle, the stronger the light intensity. Sometimes, when the light intensity is enough and there's no obstruction, a visible but vague supernumerary rainbow can be generated with a fogbow, as shown in Figure 9. The white color of the fogbow is also due to the small size of the droplet. With a very small droplet, the pattern of central maxima is very wide extending to the far first order minimum, analogous to the results from the single slit experiment. This is shown in Figure 18: the data points are severely more concentrated at first, which traces back to a larger difference with the maximum view angle at the first place. As the sunlight disperses into the light of different wavelengths, the two very wide central maxima can overlap too much to be distinguishable; while if the central maxima are narrow in the case of a droplet of a larger radius, the light of different lengths is still distinguishable from each other. In detail, whether the two over can still be distinguished is based on Rayleigh Criterion [11]. A schematic diagram is shown in Figure 19.

5.2. Remained Questions and Future Plan

Several topics are in the plan for further exploration. While the paper offers a generalized simulation upon elliptical droplets, the result of the simulation is expected to be highly dependent on the parameters (axis length, the rotational angle of the ellipse) of the droplet. And since in reality non-elliptical droplets usually do not show a unified and stabilized pattern collectively, they often do

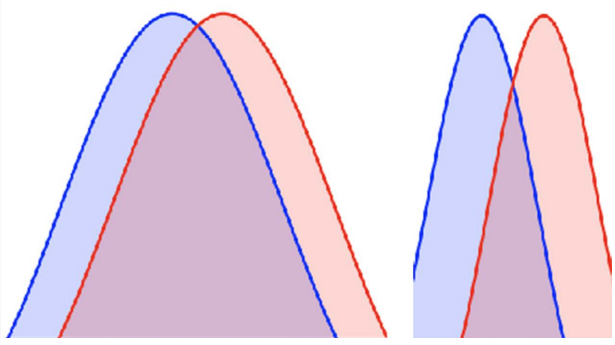

Figure 19. Contrast between the overlapping of wide and narrow central maxima.

not generate a significant visible pattern to the observer.

Also, the paper has not yet included the density and the change of density of droplets as a function of altitude, which also affects light intensity in reality. As the research goes on, more and more factors should be included in the model in order to simulate reality more precisely.

Another topic worth more discussion is the correlation between the path distance of light and the concentration of light. While the paper offers a possible explanation based on path integral, a theoretically valid solution should be further explored in future research.

Acknowledgements

The author would like to thank Prof. Riccardo Comin and Dr. Ying Xu for their valuable suggestions and discussions about the topic.

Conflicts of Interest

The author declares no conflicts of interest regarding the publication of this paper.

References

[1] Keats, J. (1990) Lamia. Woodstock Books, Oxford.

[2] Epstein, J. and Greenberg, M. (1984) Decomposing Newton's Rainbow. *Journal of The History of Ideas*, **45**, 115-140. https://doi.org/10.2307/2709334

[3] Young, T. (1845) A Course of Lectures on Natural Philosophy and the Mechanical Arts. https://doi.org/10.5962/bhl.title.27527

[4] Feynman, R.P., Leighton, R.B. and Sands, M. (2013) Optics: The Principle of Least Time. In: Feynman, R.P., Leighton, R.B. and Sands, M., Eds., *The Feynman Lectures on Physics*. Pearson PTR. https://www.feynmanlectures.caltech.edu/I_26.html#:~:text=His%20idea%20is%20this%3A%20that,which%20requires%20the%20shortest%20time

[5] Adam, J. (2002) The Mathematical Physics of Rainbows and Glories. *Physics Reports*, **356**, 229-365. https://doi.org/10.1016/S0370-1573(01)00076-X

[6] Sadeghi, I., Munoz, A., Laven, P., Jarosz, W., Seron, F., Gutierrez, D. and Jensen, H. (2012) Physically-Based Simulation of Rainbows. *ACM Transactions on Graphics*, **31**, 1-12. https://doi.org/10.1145/2077341.2077344

[7] Jackson, J. (1999) From Alexander of Aphrodisias to Young and Airy. *Physics Reports*, **320**, 27-36. https://doi.org/10.1016/S0370-1573(99)00088-5

[8] Golomb, M. (1964) Elementary Proofs for the Equivalence of Fermat's Principle and Snell's Law. *The American Mathematical Monthly*, **71**, 541-543. https://doi.org/10.2307/2312599

[9] Lubarda, V. and Talke, K. (2011) Analysis of the Equilibrium Droplet Shape Based on an Ellipsoidal Droplet Model. *Langmuir*, **27**, 10705-10713. https://doi.org/10.1021/la202077w

[10] Droplet Size: What to Understand about the Measuring Methods (2019). https://www.ikeuchi.eu/news/measurement-of-droplet-size/

[11] Tamburini, F., Anzolin, G., Umbriaco, G., Bianchini, A. and Barbieri, C. (2006) Overcoming the Rayleigh Criterion Limit with Optical Vortices. *Physical Review Letters*, **97**, 163903. https://doi.org/10.1103/PhysRevLett.97.163903